



Cite this: *Chem. Sci.*, 2021, **12**, 5672

All publication charges for this article have been paid for by the Royal Society of Chemistry

Boosting PLA melt strength by controlling the chirality of co-monomer incorporation†

An Sofie Narmon, ^a Annelies Dewaele, ^a Kevin Bruyninckx, ^a Bert F. Sels, ^a Peter Van Puyvelde ^b and Michiel Dusselier ^{a*}

Bio-based and degradable polymers such as poly(lactic acid) (PLA) have become prominent. In spite of encouraging features, PLA has a low melt strength and melt elasticity, resulting in processing and application limitations that diminish its substitution potential *vis-a-vis* classic plastics. Here, we demonstrate a large increase in zero shear viscosity, melt elasticity, elongational viscosity and melt strength by random co-polymerization of lactide with small amounts, *viz.* 0.4–10 mol%, of diethylglycolide of opposite chiral nature. These enantiomerically pure monomers can be synthesized using one-step zeolite catalysis. Screening of the ester linkages in the final PLA chains by the ethyl side groups is suggested to create an expanding effect on the polymer coils in molten state by weakening of chain–chain interactions. This effect is suspected to increase the radius of gyration, enabling more chain entanglements and consequently increasing the melt strength. A stronger melt could enable access to more cost-competitive and sustainable PLA-based biomaterials with a broader application window. Amongst others, blow molding of bottles, film blowing, fiber spinning and foaming could be facilitated by PLA materials exhibiting a higher melt strength.

Received 4th January 2021
Accepted 2nd March 2021

DOI: 10.1039/d1sc00040c
rsc.li/chemical-science

Introduction

Biobased and biodegradable polymers are appealing alternatives for petroleum-based plastics, as the latter are associated with environmental pollution, triggering worldwide public concern.^{1–3} Poly(lactic acid) (PLA), an aliphatic polyester made up of carbohydrate-sourced lactic acid (LA) monomers, is nowadays one of the most promising bioplastics on the market.^{4,5} PLA is biodegradable under industrial composting conditions and exhibits adequate mechanical and physical properties, comparable with those of commodity plastics such as polystyrene and poly(ethylene terephthalate).^{6–8}

Certain factors restrain the adoption of PLA. At present, high-molecular weight PLA is synthesized by ring-opening polymerization (ROP) of the dilactone, lactide (LD), which is made by back-biting depolymerization of polycondensed LA.^{4,9} While dilactones and ROP are indispensable, making LD is a two-step, time and energy consuming process that requires

additional purification, driving up the cost of production. Moreover, LD yields are mediocre and the process is confronted with racemization, losing control over the enantiopurity of (L,L)-lactide (L-LD), and thus of PLA.^{10,11} Recently, some of us developed a zeolite-based catalytic process, enabling the single-step conversion of LA to LD. The highly selective route outperforms the two-step procedure, potentially in cost and certainly in atom efficiency (few side-products) and in preserving stereochemistry (no racemization).¹² Other routes to lactide are also being developed and gear toward solving the cost issue.^{13–15} A more intrinsic drawback of PLA is associated with its processing performance and consequently its applicability. PLA has a poor melt strength and melt elasticity, which are crucial properties for elongational flow dominated processes such as film blowing, blow molding, fiber spinning, foaming, *etc.*^{16–18} Different strategies for improving the melt strength properties of PLA have been described. Some efforts focus on the use of chain extenders to create long chain, branched, cross-linked or star-shaped structures of PLA, to enhance chain entanglements.^{19–25} Although chain extenders can boost numerous properties of PLA, final polymer structures are often difficult to control, and seeking the optimal extender concentration remains challenging. In addition, chain extended polymer structures can exhibit reduced degradability,^{26–28} whereas extending agents themselves are often not biodegradable or biocompatible and in some cases are even toxic (diisocyanates). A second strategy consists of blending PLA with other polymers, as well as compounding it with different micro- or nanosized fillers (*e.g.* 5 wt%) to

^aDepartment of Microbial and Molecular Systems, Centre for Sustainable Catalysis and Engineering, KU Leuven, Celestijnenlaan 200F, 3001 Leuven, Belgium. E-mail: michiel.dusselier@kuleuven.be; Web: <https://dusselier-lab.org/>

^bDepartment of Chemical Engineering, Soft Matter, Rheology and Technology, KU Leuven, Celestijnenlaan 200F, 3001 Leuven, Belgium. E-mail: peter.vanpuyvelde@kuleuven.be

† Electronic Supplementary Information (ESI) available: Extended information about materials and methods (S1–S2), extended reading (S3–S7), and extended data in Tables S1–S6 and in Fig. S1–S18. See DOI: 10.1039/d1sc00040c



enhance its melt behavior.²⁹ However, homogeneous blends or equal particle dispersion are not readily obtained. Moreover, blending can result in recycling or (bio)degradation limitations.³⁰

Finally, stereocomplex crystallites, induced by mixing PLAs of opposite chiral nature (*l*-PLA with 5 wt% *d*-PLA), can act as crosslinking points, resulting in a melt behavior similar to that of chain-extended PLA structures.³¹⁻³³ However, synthesis of *d*-PLA requires large scale availability of pure *d*-LA, which is currently not trivial.³⁴ In contrast to these strategies, studies linking the composition of the backbone (linear lactide-based co-polymers) to rheological properties are scarce, despite the obvious value of microstructure – viscoelasticity relations for these polyesters. One group performed a few rheological studies on syndio- and heterotactically enriched PLAs.³⁵ The effect of incorporating *d*-LD in *l*-PLA has been a topic of investigation but without unambiguously clarifying the impact of the *D/L* ratio or showing a negligible change in polymer melt viscosity.^{36,37}

Here, we describe the unprecedented improvement of melt strength behavior of PLA by ring-opening co-polymerization of LD in the presence of (small amounts of) diethylglycolide (EG) of opposite chiral nature (Fig. 1A). Although diethylglycolide has been polymerized before, its traditional synthesis is homogeneously catalyzed, inefficient and laborious, ending up with a mixture of diastereomers.³⁸⁻⁴⁰ Zeolite-based cyclization of α -hydroxy acids here not only generates efficiency and high

yields, but also essentially maintains the full stereochemistry of the substrate, which is of utmost importance for this research. Access to enantiomerically pure cyclic ester monomers enables the exploration of a wide range of high-molecular weight (co)-polymers with possibly attractive new properties.

In this research, rheological studies on co-polymers of enantiomerically pure LD and EG revealed a strong increase in melt elasticity and melt strength compared to those of conventional PLA, with clearly observed differences associated with the chiral nature of the monomers. While improvements in melt properties are usually obtained through chain extension, blending or compounding, a simple co-polymerization here suffices, even for small EG incorporation. A promising strategy for large scale implementation thus arises, given the ease of dropping-in 1% of EG into the lactide batch for classic L-PLA production. The gains in melt strength could translate into lower weight of plastic needed per functional item (e.g. blow molding a thinner bottle) and expand the application horizon for PLA.

Experimental

Synthesis of diethylglycolide

In a typical reaction, 0.01 mol of (L)- or (D)- α -hydroxybutyric acid and 0.5 g of H-beta zeolite ($\text{SiO}_2/\text{Al}_2\text{O}_3 = 25$ or 150, (Zeolyst and Südchemie)) are added to a round bottom flask with 20 mL of

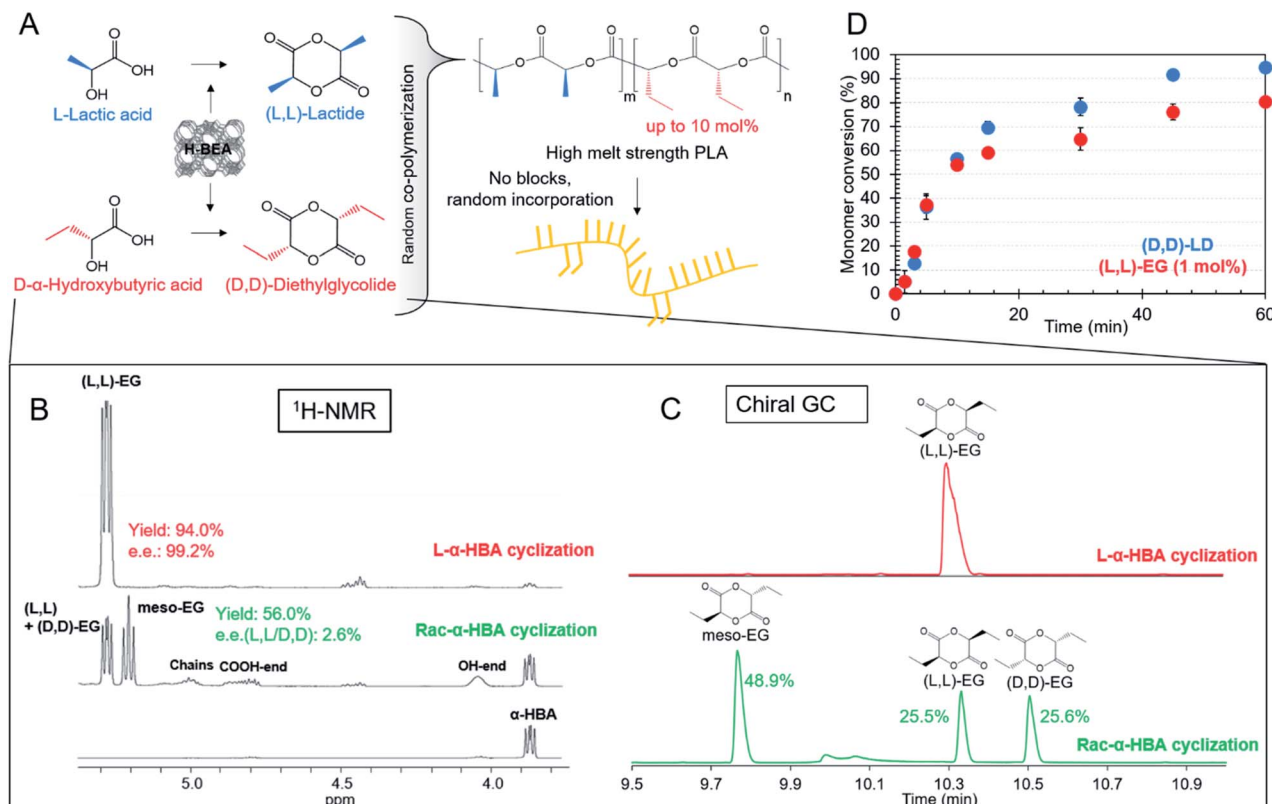


Fig. 1 (A) Catalytic one-step synthesis of diethylglycolide (EG) and random co-polymerization with lactide (LD) toward high melt strength PLA. (B) $^1\text{H-NMR}$ (400 MHz, dmso-d_6) results from catalytic cyclization of L- α -HBA and rac- α -HBA, resulting in an EG yield of 94.0% (e.e. = 99.2%) and 56.0% (e.e. = 2.6%), respectively. (C) Chiral GC results from catalytic cyclization of L- α -HBA and rac- α -HBA, showing the absence of racemization and pure (L,L)-EG and a statistical mixture of (L,D), (D,D) and meso-EG, respectively. (D) Monomer conversion (%) of (D,D)-LD and 1 mol% of (L,L)-EG over 60 minutes of polymerization (bulk, 170 °C, $\text{Sn}(\text{Oct})_2$ (monomer : catalyst = 489), 1-dodecanol (initiator : catalyst = 0.7).

toluene or *o*-xylene. On top of the round bottom flask, a custom made Dean–Stark trap, filled with solvent, is installed. The setup is connected to a condenser, and heated in an oil bath at 130 or 170 °C. The mixture is stirred for 3 hours. After the reaction, the mixture is homogenized by the addition of 15 mL of acetonitrile. After homogenization, the zeolite is removed by filtration over a glass frit filter under vacuum, and rinsed with another 10 mL of acetonitrile.

Ring-opening polymerization

Solvent-free ring-opening polymerization is carried out in a dry, custom-made round-bottom flask. In a typical experiment, a desired amount of monomer is added to a flask in an oxygen and moisture free environment. A solution of stannous octoate in toluene as a catalyst (monomer : catalyst = 2500 : 1) and 1-dodecanol as an initiator (70 mol% of the catalyst) are added to the monomer. The solvent is removed *in vacuo* and the flask is filled with argon and immersed in an oil bath at 170 °C for 70 minutes. After polymerization, the flask is cooled, and the polymer is dissolved in chloroform. The synthesized polymers are separated from the remaining monomers and oligomers *via* precipitation in methanol, filtered, and dried under reduced pressure.

Small amplitude oscillatory shear

Small amplitude oscillatory shear (SAOS) measurements are carried out on an AresMets rheometer, using a parallel plate set-up (8 mm diameter) surrounded by a convection oven, purged with N₂ gas. Prior to rheology measurements, the polymer samples are compression molded into discs of 8 mm diameter and a thickness of 1 mm. The polymer discs are vacuum dried overnight at 80 °C prior to SAOS measurements. First, dynamic time sweep measurements are performed to verify the thermal stability of the polymer samples under the applied test method. The changes in G' and G'' are determined over time at an angular frequency of 10 rad s⁻¹, a strain amplitude of 1% and a temperature of 185 °C during 300 s. Secondly, strain sweep tests are performed by varying the strain amplitude between 0.1 and 10% to determine the linear visco-elastic regime of the materials. Frequency sweep measurements are carried out at 185 °C with dynamic frequencies ranging from 0.1 to 100 rad s⁻¹ at a strain amplitude of 1–10%. Consecutively, rate sweep tests are performed applying shear rates between 0.01 and 1 s⁻¹. At each shear rate a waiting time of 30 s is installed to guarantee steady state, while a measuring time of 10 s is applied.

Extensional viscosity fixture

Extensional flow properties of the polymers are determined on an AresMets rheometer, using an Extensional Viscosity Fixture (EVF) set-up. Extensional viscosities are measured in strain-controlled stretch experiments with a Hencky strain of 3.4 at 185 °C in a N₂ atmosphere. The polymer samples are compression molded into rectangular plates of 18.0 mm long, 10.0 mm (\pm 0.10 mm) wide and 0.80 mm (\pm 0.05 mm) thick. Prior to stretch measurements, the plates are dried at 80 °C

overnight. The experimental protocol consists of three steps. During the first step a pre-stretch with a stretch rate of 0.0075 s⁻¹ is performed on the polymers to compensate for thermal expansion during heating. Before pre-stretch, a delay time of 50.0 s is applied to ensure that the polymer samples are completely molten. The pre-stretch is followed by a relaxation step of 5.0 s to remove the residual stress in the sample. Finally, the stretch measurement was performed at a constant Hencky strain rate (0.1, 0.5, 1, and 3.5 s⁻¹).

Haul-off

To determine the extensional properties of the polymer melts, a Göttfert 2002 capillary heometer is used in combination with a Haul-off apparatus. The polymer material is added to the barrel of the capillary rheometer at 185 °C. To create molten polymer strands, the melt is pushed out of the barrel by the piston with a diameter of 12 mm and a die of 2 mm at a piston speed of 0.05 mm s⁻¹. The molten strands are attached to the Haul-off apparatus which spins the molten strands on a wheel, rotating at a pull-off speed of 100 mm s⁻¹. The speed is linearly increased at an acceleration of 0.12 mm s⁻¹ till the polymer melt breaks.

Results

Catalytic monomer synthesis and co-polymerization

The scope of the one-step catalytic conversion of lactic acid (LA) to lactide (LD) in the presence of Brønsted acidic zeolite beta (H-BEA) is extended towards the cyclization of α -hydroxybutyric acid (α -HBA) to form diethylglycolide (EG). A complete overview of all catalytic syntheses of symmetric and asymmetric cyclic esters can be found in the ESI (Tables S1–S2 and Fig. S1†). Applying the same reaction conditions to L- α -HBA as those applied to L-LA by Dusselier *et al.*¹² (130 °C, 3 h, toluene, H-BEA (SiO₂/Al₂O₃ = 25)) only yielded 5% L-EG, compared to 78% for L-LD. This could be overcome by increasing the reaction temperature to 170 °C (*o*-xylene, yield = 76%), indicating a reactivity difference between LA and α -HBA. The catalyst-free reactions revealed – next to the expected low cyclic ester selectivity – a conversion decline with increasing steric hindrance of the alkyl chains at the α -position (see Fig. S2† for more details comparing the four different substrates). This confirms a slower spontaneous condensation (reactivity) of α -HBA compared to LA. In this regard, one could expect that α -HBA would tend to form smaller products and perhaps favor ring-closure. Nonetheless, a reaction with a soluble acid catalyst (sulphuric acid) at full monomer conversion yielded less than 5% EG, indicating the need for confining the acid function in a shape-selective catalyst such as H-BEA. Under optimized conditions, the zeolite reaction (with H-BEA, SiO₂/Al₂O₃ = 150) proceeded even faster and was more selective towards (L,L)-diethylglycolide (L-EG) (yield = 88%). Distillation of the α -HBA substrate before reaction yielded 94% L-EG in a single step. In addition, ¹H-NMR showed an excellent enantiomeric purity of 99.6% L-EG (e.e. = 99.2%) with formation of only 0.4% *meso*-EG (= (L,D)-EG). In



contrast to enantiopure α -HBA, racemic α -HBA (rac- α -HBA) conversion is slower and less selective (yield = 56%) for cyclic esters, but still a statistical mixture of the L,L; D,D- and L,D-diastereomers is achieved confirming the absence of racemization *via* the direct zeolite-catalyzed route (Fig. 1(B) and (C)). After the reaction, the heterogeneous catalyst is easily removed and cyclic esters are separated from the linear oligomers and unreacted monomers by phase extraction. Subsequent crystallization leads to an overall EG purity of 99.5% (e.e. \approx 100%) and an overall isolated yield of 48% (Fig. S3 \dagger). Obtaining higher isolated yields should be possible, but this was not the scope here as purity for ring-opening polymerization (ROP) was the main concern.

ROP, based on the work by Fisher *et al.*⁴¹ was performed with the stannous octanoate ($\text{Sn}(\text{Oct})_2$) catalyst and *n*-dodecanol initiator. This catalytic system ensures preservation of the stereochemistry of the monomers within the polymer chains, high molecular weight and low polydispersity.^{42,43} Diverse lactide-based polyesters were synthesized with different incorporations of EG, varying between 0.3 and 10 mol%, *i.e.* $n/(m+n)$ in Fig. 1(A). The polymers vary in stereochemistry of the co-monomers (L-EG or D-EG with L-LD or D-LD, Fig. S4 \dagger). $^1\text{H-NMR}$ proved successful incorporation of the co-monomers in polylactide (Fig. S5 \dagger), and weight-average molecular weights (M_w s) varied between 101 and 149 kg mol $^{-1}$ (Tables 1 and S3 \dagger have a full dataset). Various benchmarks were synthesized, *i.e.* a co-polymer of L-LD with

Table 1 Results of co-polymerization of L(D)-LD with D-LD or L(D)-EG by ROP, weight-average molecular weight (M_w) (kg mol $^{-1}$) and polydispersity (D) determined by GPC, T_g and T_m (°C) determined by DSC and zero shear viscosity η_0 (Pa s) and angular frequency at cross-over of G' and G'' ω_c (rad s $^{-1}$) determined by SAOS

Polymer	Schematic chain structure	Build-in ^a %	GPC		DSC		SAOS	
		Co-monomer	M_w ^b (kg mol $^{-1}$)	D	T_g (°C)	T_m (°C)	η_0 (kPa s)	ω_c (rad s $^{-1}$)
P(L-LD)		—	135	1.7	58	177	9.7	62.9
P(D-LD)		—	117	1.7	57	179	12.1	84.5
PLA Ingeo 7001D ^c	—	—	83.3	1.5	58	149	5.9	>100
P(L-LD-co-D-LD)		10 ^e	128	1.7	54	—	4.8	>100
P(L-LD-co-L-EG) 1		9.0	146	1.6	43	148	8.3	>100
P(L-LD-co-L-EG) 2		0.7	133	1.4	54	177	23.1	46.7
P(L-LD-co-D-EG) 1		10.3	101	1.4	46	127	15.2	80.4
P(L-LD-co-D-EG) 2		1.2	115	1.7	56	169	143.3	7.83
P(L-LD-co-D-EG) 3		0.7	138	1.6	54	170	33.9	32.1
P(L-LD-co-D-EG) 4		0.4	128	1.8	57	165	54.8	24.3
P(D-LD-co-D-EG) 1		0.6	142	1.6	56	170	27.8	32.7
P(D-LD-co-L-EG) 1		10.5	131	1.7	45	118	71.8	19.1
P(D-LD-co-L-EG) 2		4.1	129	1.7	54	154	108.2	8.17
P(D-LD-co-L-EG) 3		2.0	149	1.3	56	160	17.3	51.0
P(D-LD-co-L-EG) 4		1.2	118	1.7	56	171	33.3	24.3
P(D-LD-co-L-EG) 5		0.7	128	1.5	58	172	191.1	6.64
P(D-LD-co-L-EG) 6		0.3	129	1.6	56	177	22.9	76.6
Large scale reactions^d		—	—	—	—	—	—	—
P(L-LD)	—	—	106	1.6	52	177	7.1	>100
P(L-LD-co-D-EG)	—	1.2	119	1.9	59	170	14.8	55.9

^a Average build-in % of methyl and methine protons (when both visible), determined by $^1\text{H-NMR}$ (400 MHz, CDCl_3). ^b Polystyrene standards were used to calibrate weight-average molecular weights (M_w). The experimental molecular weight was corrected considering the Mark–Houwink parameters for PLA, and the same parameters are used as an estimation for the different co-polymers.⁶ ^c Commercial grade PLA from NatureWorks. ^d Large scale polymerization reactions (50–100 g). ^e Added amounts before reaction; L- and D-LD cannot be distinguished from each other in $^1\text{H-NMR}$.



10 mol% *D*-LD and pure poly(*L*-lactide) (P(*L*-LD)) and poly(*D*-lactide) (P(*D*-LD)), or purchased. The latter, a commercial PLA (Ingeo 7001D, NatureWorks) has specifications targeting use in injection stretch blow molded bottle applications.

Chain structures of co-polymers are well-known to be dependent on the relative polymerization rates of the different monomers. If propagation rates are comparable, random chain structures are obtained, whereas a significant rate difference leads to block co-polymers. Various researchers have described the decrease in the polymerization rate of alkyl-substituted lactides with increasing steric hindrance of the substituents^{38,39,44–46}. This has been attributed to a more difficult nucleophilic attack of the initiator.^{38,46} In addition, a decreased polymerisability is observed with increased intramolecular steric repulsion in the polymer chains (less present in the cyclic di-esters) which decreases the polymerization enthalpy.⁴⁴ Nevertheless, the difference in the polymerization rate between *rac*-LD and *rac*-EG has been described by Baker *et al.* as rather small when comparing the reactivity ratios, indicating a high degree of randomness within their co-polymer chains.^{38,39} Here, the randomness of incorporation was quasi confirmed by determining the time evolution of the co-monomers during ROP (Fig. 1(D); Table S4 and Fig. S6†). Only insubstantial differences in the relative progression of the conversions are detected. *L*-EG polymerization progresses (relative to its starting amount of 1%) only slightly slower than *D*-LD polymerization (99%), most probably giving rise to strongly randomized co-polymers (note that the degree of randomness can vary with the co-monomer ratio).

Differences in the thermal properties of the various co-polymers are observed. In general, a downward trend in glass transition temperature (T_g), melt temperature (T_m) and degree of crystallinity (χ_c) is obtained with increasing amounts of EG co-monomer (see Tables 1 and S3, and Fig. S7†). T_m and χ_c show a stronger decrease when co-monomers with opposite stereochemistry are used. Baker *et al.*⁴⁷ explained the decrease in T_g of poly(alkyl glycolide) polymers with alkyl side chains of increasing length (2–8 carbons) compared to that of polylactide based on weaker dipole–dipole interactions between polyester chains as due to a stronger screening of the ester groups by the alkyl side chains and thus less chain–chain interactions. The decrease in T_m and χ_c is explained by the introduction of defects in the regular structure of P(*L*- or *D*-LD), preventing chains from folding into close crystalline structures. This effect is expected to be stronger when co-monomers with opposite stereochemistry are used.⁴

Melt rheology

Shear rheology. Melt rheological properties of polymers govern their flow behavior during processing toward various applications. Processing of PLA remains challenging due to its low melt strength and melt elasticity, hampering its applicability.¹⁶ Measuring the elasticity through the elastic modulus (G') of the melt *via* strain controlled small amplitude oscillatory shear (SAOS) rheometry, can indirectly give an idea about melt strength, defined as the maximum extensional stress that can be applied to a polymer melt. SAOS measurements were

performed on the co-polymers described in Table 1, at 185 °C and a constant strain of 1% under nitrogen, to determine the modulus of complex viscosity ($|\eta^*|$), and the elastic (G') and viscous (G'') moduli with changing angular frequencies (ω) between 0.1 and 100 rad s^{−1}. The zero shear viscosity (η_0), being the plateau value of the complex viscosity at infinitely small ω , is determined by application of the Carreau–Yasuda model (see S7.1† for more details) and depicted in Tables 1 and S6.† η_0 is directly associated with the extensional viscosity (η_e) of the material under extensional deformation by the Trouton ratio ($\eta_e = 3\eta_0$).⁴⁸ The melt elasticity of the materials is determined by looking at the angular frequency at cross-over of G' and G'' (ω_c (rad s^{−1})) (Table 1). The lower the ω_c , the longer the relaxation time and the more elastic the polymer melt. The results of SAOS of the co-polymers containing 9–10% co-monomers are depicted in Fig. 2(A–C), while the same data for co-polymers with 0.6–0.7 mol% EG are depicted in Fig. 2(D–F).

All polymer melts tend to a Newtonian plateau at low frequencies, while shear-thinning occurs at higher frequencies (Fig. 1(A) and (D)). Several observations emerge from the data by comparing the viscoelastic properties of the co-polymers with those of P(*L*-LD), a self-made control with a similar M_w , and the commercial grade PLA (Ingeo) designed for injection stretch blow molding. Adding 10 mol% of *D*-LD to P(*L*-LD) seems to decrease the viscosity and elasticity of pure P(*L*-LD) to a small extent, in line with earlier studies noting only subtle differences in the viscoelastic properties of polylactides with various *D*-LD contents.^{36,37,49} While the viscoelastic properties do not seem to significantly change with incorporation of 10 mol% *L*-EG in P(*L*-LD), co-polymers with 10 mol% EG and LD with opposite stereochemistry exhibit remarkable increases in both complex viscosity and elasticity of the polymer melts (Fig. 2(A–C) and Table 1). While the average η_0 of P(*L*-LD) and P(*D*-LD) (Table S6†) is calculated to be 12 324 Pa s (standard deviation of 7585 Pa s) and the average ω_c lies around 72 rad s^{−1}, for an average M_w of 122.5 kg mol^{−1}, the values of P(*L*-LD-co-*D*-EG) and P(*D*-LD-co-*L*-EG) are estimated to be 15 212 ($\omega_c = 80.4$ rad s^{−1}) and 71 783 Pa s ($\omega_c = 19.1$ rad s^{−1}), respectively (Carreau–Yasuda model, see S7.1† for more details). Since the melt viscosity and elasticity are strongly dependent on the chain length,^{19,50} one could argue that the increase in P(*L*-LD-co-*D*-EG) is limited due to its rather low M_w (101 kg mol^{−1}). Nevertheless, P(*D*-LD-co-*L*-EG) exceeds the zero shear viscosity of P(*L*-LD) with a factor 6, exhibiting a unique beneficial impact on the viscoelastic properties of polylactide. Interestingly, comparable results were obtained when much lower amounts, *viz.* 0.6–0.7 mol%, of EG were incorporated in polylactide (Fig. 2(D–F) and Table 1). Notably, co-polymers in which EG and LD have the same stereochemistry, (P(*L*-LD-co-*L*-EG) and P(*D*-LD-co-*D*-EG)) exhibited a limited increase in viscosity and elasticity, while the increase is most significant for co-polymers of *L*-LD and *D*-EG or *D*-LD and *L*-EG. To make sure effects are not largely attributable to variations in M_w , a Mark–Houwink correction was applied to the calculated zero shear viscosities shown in Table 1, which can be consulted in Fig. S16.† Note that as an estimate the same parameters were used for all different co-polymers. This correction further strengthens the possible melt-strength improving effects of EG.



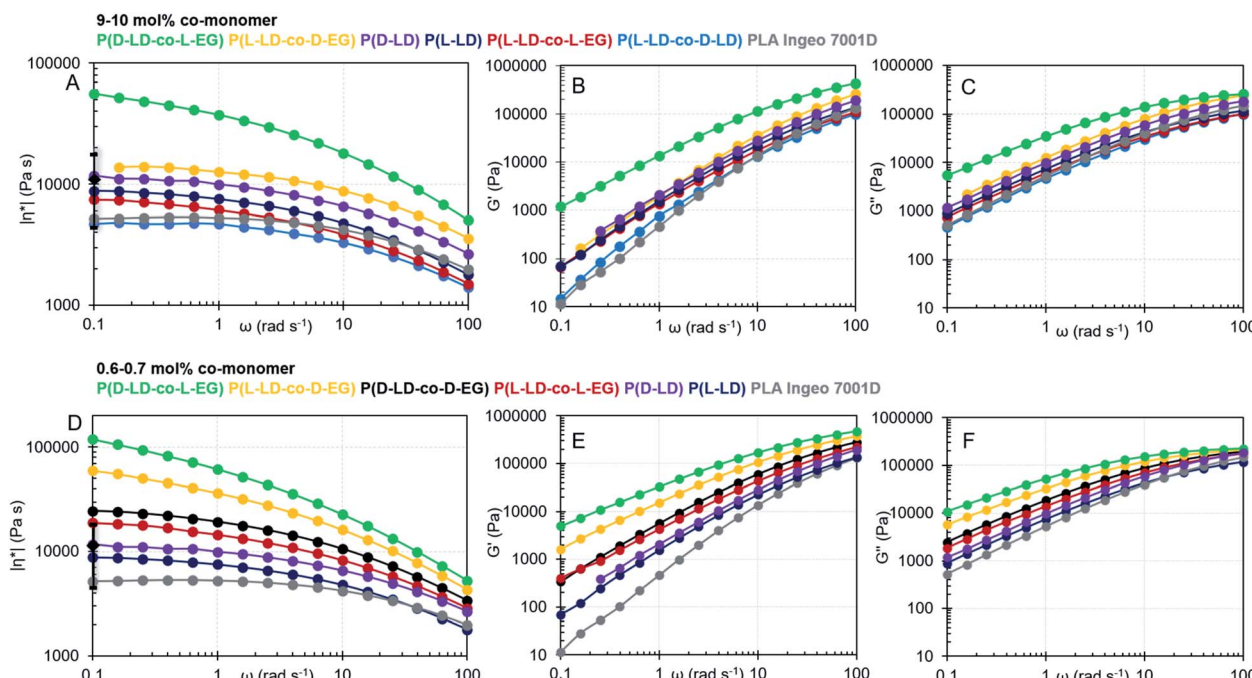


Fig. 2 (A) Complex shear viscosity ($|\eta^*|$), (B) elastic modulus (G') and (C) viscous modulus (G'') as a function of angular frequency (ω) for co-polymers with 9–10 mol% of co-monomer. (D) Complex shear viscosity ($|\eta^*|$), (E) elastic modulus (G') and (F) viscous modulus (G'') as a function of angular frequency (ω) for co-polymers with 0.6–0.7 mol% of co-monomer. \blacklozenge and error bars at 0.1 rad s^{-1} in (A) and (D) indicate the average value and standard deviation as calculated from different synthesized homopolymers of pure L or D-LD (see the ESI† for more details). The colors are also traceable in Table 1.

To study the effect of the co-monomer ratio (EG : LD) on the viscoelastic properties of the materials, various co-polymers ($\text{P}(\text{L-LD-co-D-EG})$ and $\text{P}(\text{D-LD-co-L-EG})$) with different percentages of EG were analyzed (Tables 1 and S6, and Fig. S12–S15†). It can be noticed that for both $\text{P}(\text{L-LD-co-D-EG})$ and $\text{P}(\text{D-LD-co-L-EG})$ no clear correlation exists between viscosity or elasticity and the co-monomer ratio. For $\text{P}(\text{D-LD-co-L-EG})$ rather low η_0 s and high ω_c s are observed when 0.3 or 2.0 mol% of EG is incorporated, while incorporation of 0.7, 4.1 or 10.5% exhibits a remarkable improvement in viscoelastic properties. For $\text{P}(\text{L-LD-co-D-EG})$ very high viscosity and elasticity are seen when 1.2 or 0.4% of D-EG is used. Nevertheless, the co-polymer with 10.3 mol% D-EG shows a much smaller increase, which is likely attributed to its rather low M_w compared to the other polymers. The non-directional trends potentially derive from changes in the mode of incorporation with the percentages (e.g. random vs. block) or other polymer microstructure effects. Different reactivity ratios have been reported when changing co-monomer percentages.⁵⁴ Although M_w s vary to some extent, the variation is limited and unlikely to cause such large effects (see M_w correction Fig. S16†). In addition, these effects seem to be reproducible in different co-polymers of LD and EG. Although the data described here cannot be compared to the literature data directly (due to differences in molecular weight, (D,D)-lactide content, additive mixing techniques, *etc.*), one can conclude that the zero shear viscosity values described here are in the same range as values obtained in the literature when mixing PLA with 1–3 wt% of Joncyl, a reactive additive.^{51–53}

Extensional rheology. Although shear rheometry and melt elasticity give good indications about the melt properties of the co-polymers, extensional rheometry can be used as a direct measurement of melt strength. To confirm the existence of the unusually high melt elasticities, to mitigate some of the variability of small-scale experiments, and to allow extensional rheometry (sample sizes), the bulk ROP reactions were scaled-up to 100 g. A pure $\text{P}(\text{L-LD})$ polymer and a co-polymer of L-LD with 1.2% of D-EG were synthesized (for basic polymer characteristics, see Table 1) and compared to the commercial grade PLA, *viz.* PLA Ingeo 7001D, used for injection stretch blow molding applications (*e.g.* bottles).

Extensional viscosity fixture measurements were performed at different Hencky strain rates (0.1, 0.5, 1 and 3.5 s^{-1}) to determine the extensional viscosity (η_e) as a function of extension time (time_e) (Fig. 3(A): Hencky strain rate = 3.5 s^{-1} , data at other rates can be found in the ESI (S7.2†)). Extensional viscosity is related to η_0 by a factor of three as explained using the Trouton ratio ($\eta_e = 3\eta_0$) (see S7.2† for more details).

A comparable extensional viscosity is observed for the commercial PLA grade and the synthesized $\text{P}(\text{L-LD})$ sample, while $\text{P}(\text{L-LD-co-D-EG})$ confirms its higher viscosity. Although a strong difference in viscosity is noticed, no strain hardening behavior is observed at these Hencky strain rates, in agreement with the literature on extensional viscosity of linear polylactide.^{55,56}

Finally, to directly measure the melt strength, vertical polymer melt strands (Fig. S18†) were spun on a wheel at a linearly

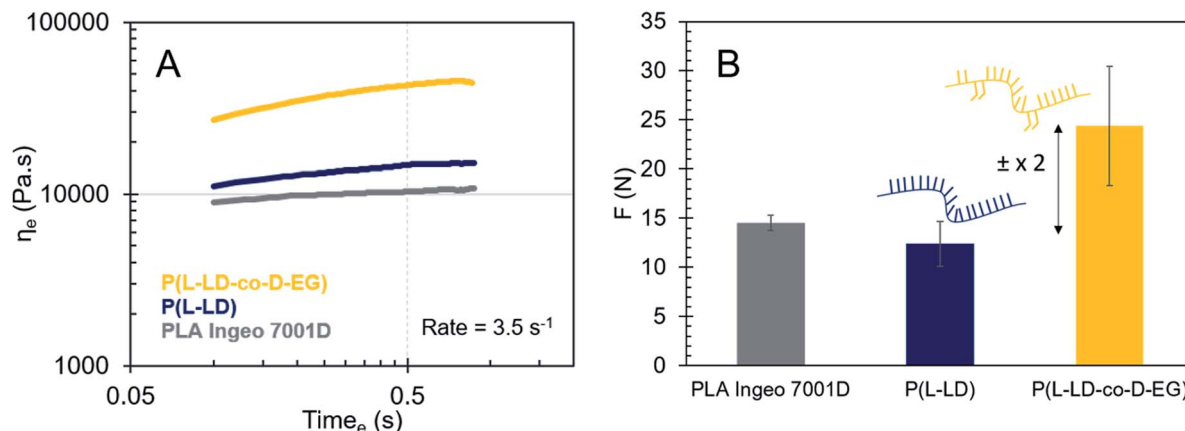


Fig. 3 Large scale extensional viscosity measurements on P(L-LD), P(L-LD-co-D-EG) (1.2 mol% D-EG) and PLA Ingeo 7001D (A) extensional viscosity (η_e) as a function of extension time (t_e) at a Hencky strain rate of 3.5 s^{-1} determined with an extensional viscosity fixture rheometer. (B) Average extensional force exerted by the polymer materials determined by using a Haul-off extensional rheometer.

accelerating velocity ($100\text{--}5000\text{ mm s}^{-1}$) and the extensional force exerted by the materials was determined using a Haul-off extensional rheometer (details in S7.3†). While strong variations were seen in the rotation speed at which the polymer materials broke, forces seemed to be quite constant. P(L-LD-co-D-EG) exhibited an average force of about 24.4 N (Fig. 3(B)), which is about two times higher than the force of P(L-LD) (12.4 N). P(L-LD) and the commercial PLA showed very comparable values. This large scale – from a polymer chemist point of view – measurement consolidates the presumption of a severe rise in the melt strength of polylactide with incorporation of small amounts of EG with opposite stereochemistry.

Discussion

Co-polymerization of LD and EG with a reverse stereo-configuration seems to uniquely impact the viscoelastic properties of PLA. While improvements in melt properties are mostly the results of chain extension, stereocomplexation, blending, compounding, *etc.*, obtaining these effects here through co-polymerization is unexpected and may open new ways to more functional PLA. A higher melt strength and melt elasticity could facilitate certain elongational dominated processes (extrusion blow molding, thermoforming, film blowing, foaming, *etc.*), broadening the application window of PLA bioplastics, simply by adding a small amount of comonomer to the existing ROP procedure. Moreover, if a thinner stretch can be achieved without breakage of the stronger melt, less polymer is required for a given application, substantially reducing the ecological footprint of the plastic application. Since the ethyl side groups, here incorporated into the polylactide backbone, are too short to induce extra side-chain entanglements,^{19,36} other explanations should be invoked and investigated for this spectacular increase in melt strength and melt elasticity.

Yamane *et al.*³² obtained indicative, but less strong, viscoelastic effects by blending small amounts of low molecular weight P(D-LD) into P(L-LD). This was explained by P(D-LD)

acting as branching points on the P(L-LD) chains, forming small stereocomplex crystallites at the contact points of P(L-LD) and P(D-LD) chains. These crystallites stay solid above the T_m of P(L-LD), counteracting disentanglement under shear deformation. Similar interactions may occur between the P(L-LD-co-D-EG) or P(D-LD-co-L-EG) chains in our co-polymers. Stereocomplexation between blends of P(L- α -HBA) and P(D-LA)⁵⁷ or P(L- α -HBA) and P(D- α -HBA)⁵⁸ as well as stereocomplexation between stereoblock co-polymers of P(D- α -HBA) and P(L-LA) (note that these are polycondensation-derived) have been described in the literature.⁵⁹ However, the ring-opening-polymerization-derived co-polymers in our work only contain very small amounts of comonomers, randomly distributed throughout the PLA chains. Moreover, no proof of stereocomplexation was observed in the DSC measurements, which should be manifested as a melting peak at higher temperatures, *i.e.* above the melting peaks of both homopolymers of LD and EG (Fig. S7†), rendering the stereocomplex hypothesis unlikely. To further ensure the absence of stereocomplex crystallites, G' and G'' values of some of the prepared co-polymers were measured at increasing temperatures up to $230\text{ }^\circ\text{C}$ to detect sudden drops in elasticity or viscosity of the materials. Since no remarkable effects were observed (Fig. S17†), presence of such crystallites with higher T_m can be discarded.

Even though the ethyl side groups are unable to foresee strong entanglements among polymer chains, their presence will likely affect the expansion of the polymer coils in molten state due to decreased inter- and intramolecular chain interactions. This effect might increase the radius of gyration (R_g) of the polymer coils (Fig. 4), rendering them more amenable to entanglements, resulting in higher elasticity and melt strength. This hypothesis agrees with the weaker chain–chain interactions between polydiethylglycolide chains compared to those in polylactide chains, as discussed above. Baker *et al.*⁴⁷ described the screening effect of alkyl side chains with increasing length (2–8 carbons) on the ester groups in poly(alkyl glycolide) polymers and decreasing T_g as a result of reduced dipole–dipole interactions between polymer chains. One can hypothesize here



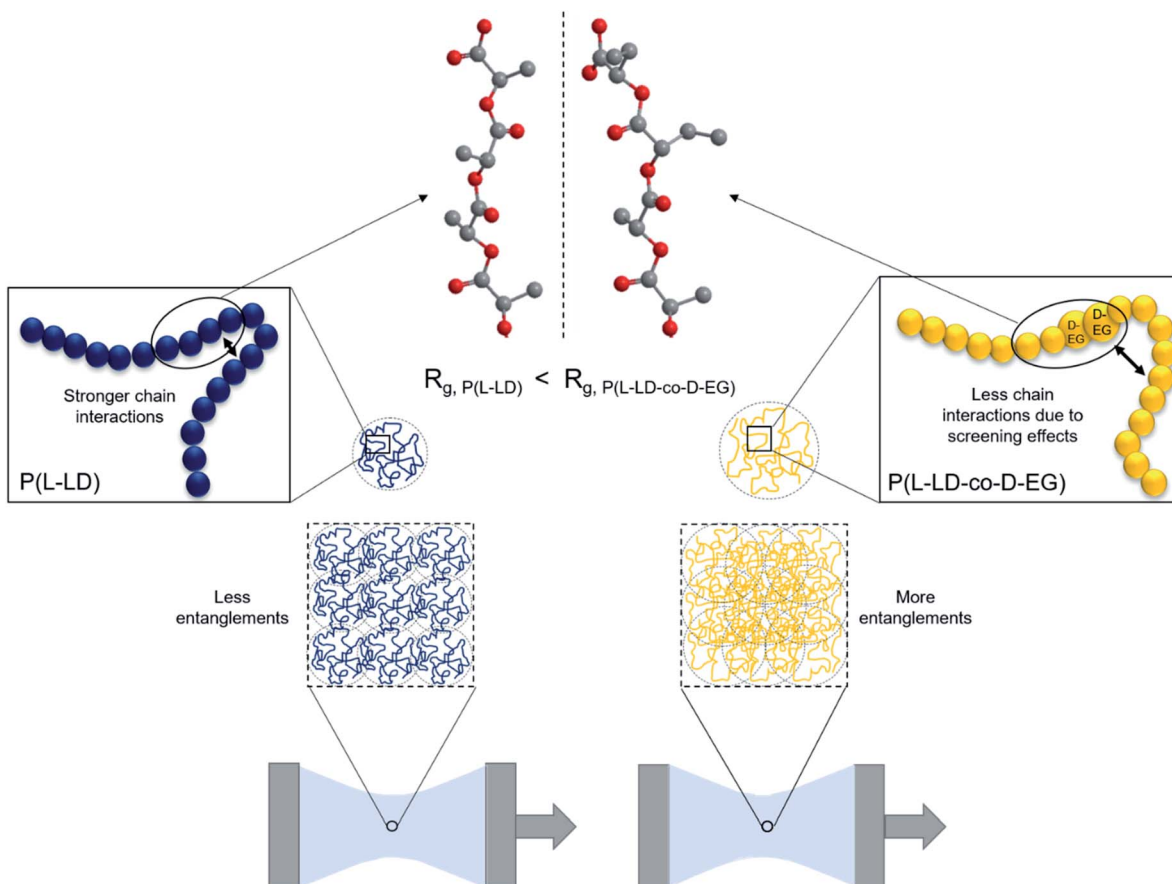


Fig. 4 Hypothesis for the observed increases in melt strength based on R_g and screening effects, and the molecular structure in the inset showing the location of the inverse enantiomer of the incorporated ethyl side group in $P(L-LD-co-D-EG)$.

that such screening effects are stronger when LD and EG are of opposite chirality, as the possibility to stack the chains is reduced. Interchain interactions are expected to dominate in polymer melts as models and theories describing polymer melt associations neglect the effects of intrachain interactions.^{60–62} However, a recent study by Carrillo *et al.*⁶³ demonstrates the importance of the often under-investigated intrachain associations or intrachain loops in determining the structure of associating polymers in the melt state and their influence on the viscoelastic properties of these materials. On the other hand, the exact relation between viscoelastic properties and radius of gyration is still under discussion.⁶⁴ This relation is described as dependent on both M_w and the density of the polymer coils in molten state. While the effect of M_w is already discussed above, the density of polymer coils is expected to be limited when dealing with very comparable polymer structures.⁶⁵

Conclusions

The one-step conversion of α -hydroxybutyric acid in the presence of zeolite H-BEA to diethylglycolide in high yields and enantiomeric purity has been shown. Access to the enantiomerically pure cyclic ester allowed us to investigate a range of unexplored high-molecular weight, random co-polymers with

lactide, exhibiting spectacular melt properties. α -Hydroxybutyric acid, the precursor to diethylglycolide, is naturally produced in mammalian hepatic tissues.⁶⁶ (Bio)chemical syntheses of this hydroxy acid are known, starting from naturally occurring compounds such as α -ketobutyric acid,⁶⁷ L-threonine,⁶⁸ alpha-aminobutyric acid⁶⁹ or methyl vinyl glycolate.⁷⁰ Although chemical syntheses by reacting butyraldehyde with NaClO or by heating α -bromobutyric acid with formamide⁷¹ are probably the main routes at the moment, biotechnological routes to obtain α -hydroxybutyric acid seem feasible. PLA co-polymers containing randomly distributed, small amounts (up to 10 mol%) of diethylglycolide, importantly of opposite chiral nature compared to lactide, result in unique polymer materials with high melt elasticity. The effect was successfully reproduced at large scale, while additional extensional viscosity measurements on the large-scale co-polymer samples confirmed the presumption of the melt strength improving effect of EG. A large scale co-polymer of (L,L)-lactide with (D,D)-diethylglycolide (1.2 mol%) exhibited an extensional viscosity and extensional force both substantially higher than those of common L-PLA. Interestingly, these values were also significantly better than those of the commercial grade PLA (Ingeo 7001D) reference, that is deliberately designed for use in injection stretch blow molding applications. It is hypothesized that the beneficial melt

elasticity effects are related to the screening role of the ethyl side groups, lowering interchain interactions and the presence of intrachain loops, and foreseeing polymer coils with a larger radius of gyration that are prone to chain entanglements. Given that this work is the first of its kind that demonstrates such effects in PLA, discarding the use of chain extenders, blending, compounding or stereocomplexation, it may lay a new foundation for unexplored pathways towards high melt strength materials *via* co-polymerization. A stronger melt can translate into less plastic usage per item, for the same functionality, thus lowering the overall ecological and economic footprint of bio-plastic items, where strong extensional forces are needed in the processing (*e.g.* during blow molding of bottles, fibre spinning, foaming, *etc.*).

Author contributions

A.D., P.V.P and M.D. initiated the research and discovered the first proofs of concept. A.S.N confirmed the proofs, elaborated most experimental findings and did large scale rheology testing. K.B. assisted with and established polymerization protocols. All authors analyzed the data. A.S.N. and M.D. wrote the manuscript with critical input by P.V.P, K.B. and B.S.

Conflicts of interest

There are no conflicts to declare. A.S.N, A.D., B.S., P.V.P and M.D. filed a European patent application on this invention.

Acknowledgements

A.D., P.V.P and M.D. acknowledge KU Leuven for a BOF-PDM grant to A.D. M.D. acknowledges KU Leuven for startup funding as BOFZAP. The authors acknowledge Corbion for kindly providing (L,L) and (D,D)-lactide.

Notes and references

- 1 J. Hammer, M. H. S. Kraak and J. R. Parsons, in *Reviews of Environmental Contamination and Toxicology*, Springer, New York, 2012, pp. 1–44.
- 2 C. Wilcox, E. Van Sebille and B. D. Hardesty, *Proc. Natl. Acad. Sci. U. S. A.*, 2015, **112**, 11899–11904.
- 3 M. Xiong, D. K. Schneiderman, F. S. Bates, M. A. Hillmyer and K. Zhang, *Proc. Natl. Acad. Sci. U. S. A.*, 2014, **111**, 8357–8362.
- 4 R. Auras, L.-T. Lim, S. E. M. Selke and H. Tsuji, *Poly(lactic acid): Synthesis, Structures, Properties, Processing, and Applications*, John Wiley & Sons, Hoboken, New Jersey, 2010.
- 5 M. Jamshidian, E. A. Tehrany, M. Imran, M. Jacquot and S. Desobry, *Compr. Rev. Food Sci. Food Saf.*, 2010, **9**, 552–571.
- 6 D. Garlotta, *J. Polym. Environ.*, 2001, **9**, 63–84.
- 7 R. E. Drumright, P. R. Gruber and D. E. Henton, *Adv. Mater.*, 2000, **12**, 1841–1846.
- 8 S. Farah, D. G. Anderson and R. Langer, *Adv. Drug Delivery Rev.*, 2016, **107**, 367–392.
- 9 S. Inkinen, M. Hakkarainen, A.-C. Albertsson and A. Södergård, *Biomacromolecules*, 2011, **12**, 523–532.
- 10 P. Gruber, *et al.*, *US Pat. 5142023*, 1992.
- 11 D. K. Yoo and D. Kim, *Macromol. Res.*, 2006, **14**, 510–516.
- 12 M. Dusselier, P. Van Wouwe, A. Dewaele, P. A. Jacobs and B. F. Sels, *Science*, 2015, **349**, 79–81.
- 13 P. P. Upare, J. W. Yoon, D. W. Hwang, U. H. Lee, Y. K. Hwang, D. Y. Hong, J. C. Kim, J. H. Lee, S. K. Kwak, H. Shin, H. Kim and J. S. Chang, *Green Chem.*, 2016, **18**, 5978–5983.
- 14 R. De Clercq, M. Dusselier, E. Makshina and B. F. Sels, *Angew. Chem.*, 2018, **57**, 3074–3078.
- 15 S. Heo, H. W. Park, J. H. Lee and Y. K. Chang, *ACS Sustainable Chem. Eng.*, 2019, **7**, 6178–6184.
- 16 L. T. Lim, R. Auras and M. Rubino, *Prog. Polym. Sci.*, 2008, **33**, 820–852.
- 17 J. Dorgan, in *Poly(lactic acid): Synthesis, Structure, Properties, Processing and Applications*, ed. H. T. Rafael Auras, Loong-Tak Lim and Susan E. M. Selke, John Wiley & Sons, New York, 2010, pp. 125–139.
- 18 M. Nofar and C. B. Park, *Prog. Polym. Sci.*, 2014, **39**, 1721–1741.
- 19 J. R. Dorgan, J. S. Williams and D. N. Lewis, *Rheol. Bull.*, 1999, **43**, 1141–1155.
- 20 A. Michalski, M. Brzezinski, G. Lapienis and T. Biela, *Prog. Polym. Sci.*, 2019, **89**, 159–212.
- 21 J. Liu, L. Lou, W. Yu, R. Liao, R. Li and C. Zhou, *Polymer*, 2010, **51**, 5186–5197.
- 22 Y. M. Corre, J. Duchet, J. Reignier and A. Maazouz, *Rheol. Acta*, 2011, **50**, 613–629.
- 23 L. Wang, X. Jing, H. Cheng, X. Hu, L. Yang and Y. Huang, *Ind. Eng. Chem. Res.*, 2012, **51**, 10731–10741.
- 24 S. Nouri, C. Dubois and P. G. Lafleur, *J. Polym. Sci., Part B: Polym. Phys.*, 2015, **53**, 522–531.
- 25 M. Mihai, M. A. Huneault and B. D. Favis, *Polym. Eng. Sci.*, 2010, **50**, 629–642.
- 26 M. A. Ghalia and Y. Dahman, *Int. J. Biol. Macromol.*, 2017, **95**, 494–504.
- 27 F. Iñiguez-Franco, R. Auras, J. Ahmed, S. Selke, M. Rubino, K. Dolan and H. Soto-Valdez, *Polym. Test.*, 2018, **67**, 190–196.
- 28 W. Limsukon, R. Auras and S. Selke, *Polym. Test.*, 2019, **80**, 106108.
- 29 M. Nofar, R. Salehiyan and S. Sinha Ray, *Polym. Rev.*, 2019, **59**, 465–509.
- 30 M. Murariu and P. Dubois, *Adv. Drug Delivery Rev.*, 2016, **107**, 17–46.
- 31 Y. Ikada, K. Jamshidi, H. Tsuji and S. H. Hyon, *Macromolecules*, 1987, **20**, 904–906.
- 32 H. Yamane, K. Sasai, M. Takano and M. Takahashi, *Rheol. Bull.*, 2004, **48**, 599–609.
- 33 S. Saeidlou, M. A. Huneault, H. Li and C. B. Park, *J. Appl. Polym. Sci.*, 2014, **41073**, 1–8.
- 34 P. Van Wouwe, M. Dusselier, E. Vanleeuw and B. Sels, *ChemSusChem*, 2015, **9**, 907–921.
- 35 L.-E. Chile, P. Mehrkhodavandi and S. G. Hatzikiriakos, *Macromolecules*, 2016, **49**, 909–919.
- 36 J. R. Dorgan, J. Janzen, M. P. Clayton, S. B. Hait and D. M. Knauss, *Rheol. Bull.*, 2005, **49**, 607–619.



37 N. Othman, A. Acosta-Ramírez, P. Mehrkhodavandi, J. R. Dorgan and S. G. Hatzikiriakos, *Rheol. Bull.*, 2011, **55**, 987–1005.

38 M. Yin and G. L. Baker, *Macromolecules*, 1999, **32**, 7711–7718.

39 E. Vogel, M. R. Smith III and G. L. Baker, in *Proceedings of the American Chemical Society*, 2007, p. 2.

40 K. D. Jandt and U. S. Schubert, *Polym. Chem.*, 2019, **10**, 5440–5451.

41 S. Kaihara, S. Matsumura, A. G. Mikos and J. P. Fisher, *Nat. Protoc.*, 2007, **2**, 2767–2771.

42 H. R. Kricheldorf, I. Kreiser-Saunders and C. Boettcher, *Polymer*, 1995, **36**, 1253–1259.

43 M. Ryner, K. Stridsberg, A. C. Albertsson, H. Von Schenck and M. Svensson, *Macromolecules*, 2001, **34**, 3877–3881.

44 W. Saiyasombat, R. Molloy, T. M. Nicholson, A. F. Johnson, I. M. Ward and S. Poshyachinda, *Polymer*, 1998, **39**, 5581–5585.

45 F. Jing, M. R. Smith and G. L. Baker, *Macromolecules*, 2007, **40**, 9304–9312.

46 T. Trimaille, M. Möller and R. Gurny, *J. Polym. Sci., Part A: Polym. Chem.*, 2004, **42**, 4379–4391.

47 G. L. Baker, E. B. Vogel and M. R. Smith III, *Polym. Rev.*, 2008, **48**, 64–84.

48 F. T. Trouton, *Proc. R. Soc. London, Ser. A*, 1906, **A77**, 426–440.

49 L. I. Palade, H. J. Lehermeier and J. R. Dorgan, *Macromolecules*, 2001, **34**, 1384–1390.

50 J. J. Cooper-white and M. E. Mackay, *J. Polym. Sci., Part B: Polym. Phys.*, 1999, **37**, 1803–1814.

51 N. Najafi, M. C. Heuzey, P. J. Carreau, D. Therriault and C. B. Park, *Rheol. Acta*, 2014, **53**, 779–790.

52 R. Al-ity, K. Lamnawar and A. Maazouz, *Eur. Polym. J.*, 2014, **58**, 90–102.

53 Y.-M. Corre, A. Maazouz, J. Duchet and J. Reignier, *J. Supercrit. Fluids*, 2011, **58**, 177–188.

54 M. Gagliardi and A. Bifone, *PLoS One*, 2018, **13**, 1–15.

55 A. T. Hedegaard, L. Gu and C. W. Macosko, *J. Rheol.*, 2015, **59**, 1397–1417.

56 L. Gu, Y. Xu, G. W. Fahnhorst and C. W. Macosko, *J. Rheol.*, 2017, **61**, 785–796.

57 H. Tsuji, S. Yamamoto, A. Okumura and Y. Sugiura, *Biomacromolecules*, 2010, **11**, 252–258.

58 H. Tsuji and A. Okumura, *Macromolecules*, 2009, **42**, 7263–7266.

59 H. Tsuji, K. Shimizu, Y. Sakamoto and A. Okumura, *Polymer*, 2011, **52**, 1318–1325.

60 M. Rubinstein and A. N. Semenov, *Macromolecules*, 2001, **34**, 1058–1068.

61 W. C. Forsman, *Macromolecules*, 1982, **15**, 1032–1040.

62 L. G. Baxandall, *Macromolecules*, 1989, **22**, 1982–1988.

63 J. Y. Carrillo, W. Chen, Z. Wang, B. G. Sumpter and Y. Wang, *J. Phys. Commun.*, 2019, **3**, 1–6.

64 D. E. Dunstan, *Sci. Rep.*, 2019, **9**, 1–9.

65 L. J. Fetters, D. J. Lohse, D. Richter, T. A. Witten and A. Zirkel, *Macromolecules*, 1994, **27**, 4639–4647.

66 W. E. Gall, K. Beebe, K. A. Lawton, K.-P. Adam, M. W. Mitchell, P. J. Nakhle, J. A. Ryals, M. V. Milburn, M. Nannipieri, S. Camastra, A. Natali and E. Ferrannini, *PLoS One*, 2010, **5**, 1–11.

67 M.-J. Kim and G. M. Whitesides, *J. Am. Chem. Soc.*, 1988, **110**, 2959–2964.

68 P. Yao, Y. Cui, S. Yu, Y. Du, J. Feng, Q. Wu and D. Zhu, *Adv. Synth. Catal.*, 2016, **358**, 2923–2928.

69 H. Tsuji, K. Nakayama and Y. Arakawa, *RSC Adv.*, 2020, **10**, 39000–39007.

70 A. Sølvhøj, E. Taarning and R. Madsen, *Green Chem.*, 2016, **18**, 5448–5455.

71 K. Miltenberger, in *Ullmann's Encyclopedia of Industrial Chemistry*, 2012, pp. 481–491.

